Biochemical Pharmacology 80 (2010) 170–178

Contents lists available at ScienceDirect

Biochemical Pharmacology

journal homepage: www.elsevier.com/locate/biochempharm

Syrbactin class proteasome inhibitor-induced apoptosis and autophagy occurs in association with p53 accumulation and Akt/PKB activation in neuroblastoma

Crystal R. Archer [a,b,1], Dana-Lynn T. Koomoa [a,1], Erin M. Mitsunaga [a,c], Jérôme Clerc [d], Mariko Shimizu [a], Markus Kaiser [d], Barbara Schellenberg [e], Robert Dudler [e], André S. Bachmann [a,b,c,*]

[a] Cancer Research Center of Hawaii, University of Hawaii at Manoa, 1236 Lauhala Street, Honolulu, HI 96813, USA
[b] Department of Cell and Molecular Biology, John A. Burns School of Medicine, University of Hawaii at Manoa, 651 Ilalo Street, Honolulu, HI 96813, USA
[c] Department of Molecular Biosciences and Bioengineering, University of Hawaii at Manoa, 1955 East-West Road, Honolulu, HI 96822, USA
[d] Chemical Genomics Centre der Max-Planck-Gesellschaft, Otto-Hahn-Str. 15, 44227 Dortmund, Germany
[e] Zürich-Basel Plant Science Center, Institute of Plant Biology, University of Zürich, Zollikerstr. 107, 8008 Zürich, Switzerland

ARTICLE INFO

Article history:
Received 13 January 2010
Accepted 25 March 2010

Keywords:
Apoptosis
Autophagy
Neuroblastoma
Proteasome inhibitors
Syrbactins

ABSTRACT

Syrbactins belong to a new class of proteasome inhibitors which include syringolins and glidobactins. These small molecules are structurally distinct from other, well-established proteasome inhibitors, and bind the eukaryotic 20S proteasome by a novel mechanism. In this study, we examined the effects of syringolin A (SylA) and glidobactin A (GlbA) as well as two synthetic SylA-analogs (SylA-PEG and SylA-LIP) in human neuroblastoma (SK-N-SH), human multiple myeloma (MM1.S, MM1.RL, and U266), and human ovarian cancer (SKOV-3) cells. While all four syrbactins inhibited cell proliferation in a dose-dependent manner, GlbA was most potent in both dexamethasone-sensitive MM1.S cells (IC_{50}: 0.004 μM) and dexamethasone-resistant MM1.RL cells (IC_{50}: 0.005 μM). Syrbactins also inhibited the chymotrypsin-like proteasome activity in a dose-dependent fashion, and GlbA was most effective in SK-N-SH cells (IC_{50}: 0.015 μM). The GlbA-promoted inhibition of proteasomal activity in SK-N-SH cells resulted in the accumulation of ubiquitinated proteins and tumor suppressor protein p53 and led to apoptotic cell death in a time-dependent manner. GlbA treatment also promoted the activation of Akt/PKB via phosphorylation at residue Ser^{473} and induced autophagy as judged by the presence of the lipidated form of microtubule-associated protein 1 light chain 3 (LC3) and autophagosomes. Collectively, our data suggest that syrbactins belong to a new and effective proteasome inhibitor class which promotes cell death. Proteasome inhibition is a promising strategy for targeted anticancer therapy and syrbactins are a new class of inhibitors which provide a structural platform for the development of novel, proteasome inhibitor-based drug therapeutics.

1. Introduction

The human proteasome is a multi-protein complex that is responsible for the degradation of a large number of proteins that regulate cell division, proliferation, and apoptosis [1,2]. Proteasome inhibitors cause selective apoptosis of malignant cells in cell culture and pre-clinical models and represent a new family of anti-neoplastic agents [3–6]. Most prominently, bortezomib (Velcade®, formerly known as PS-341) is the first proteasome inhibitor approved by the U.S. Food and Drug Administration (FDA) for the treatment of refractory and/or relapsed multiple myeloma (MM) and mantle cell lymphoma. The potential efficacy of bortezomib alone and in combination with chemotherapeutic or biologically targeted drugs is currently evaluated in several adult cancer clinical trials and a small number of pediatric cancer trials (*e.g.*, neuroblastoma) [7,8]. For example, bortezomib was recently approved for the treatment of newly diagnosed myeloma in combination with melphalan and prednisone. Despite the undisputable success with bortezomib, issues regarding bortezomib resistance, inhibitor specificity, and toxicity-associated adverse effects have emerged [9]. Therefore, other, structurally distinct proteasome inhibitors are desirable to expand the existing drug platform and to generate novel types of proteasome inhibitors which may also become useful in the treatment of bortezomib-resistant tumors.

We have recently reported the discovery of a new proteasome inhibitor class, the syrbactins, which bind the eukaryotic proteasome by a novel mechanism [10]. Syrbactins, including syringolin A (SylA) and glidobactin A (GlbA) (Fig. 1), are small molecule

* Corresponding author at: Cancer Research Center of Hawaii, Natural Products and Cancer Biology Program, University of Hawaii at Manoa, 1236 Lauhala Street, Honolulu, HI 96813, USA. Tel.: +1 808 586 2962; fax: +1 808 586 2970.
E-mail address: abachmann@crch.hawaii.edu (A.S. Bachmann).
[1] These authors contributed equally to this work.

0006-2952/$ – see front matter © 2010 Elsevier Inc. All rights reserved.
doi:10.1016/j.bcp.2010.03.031

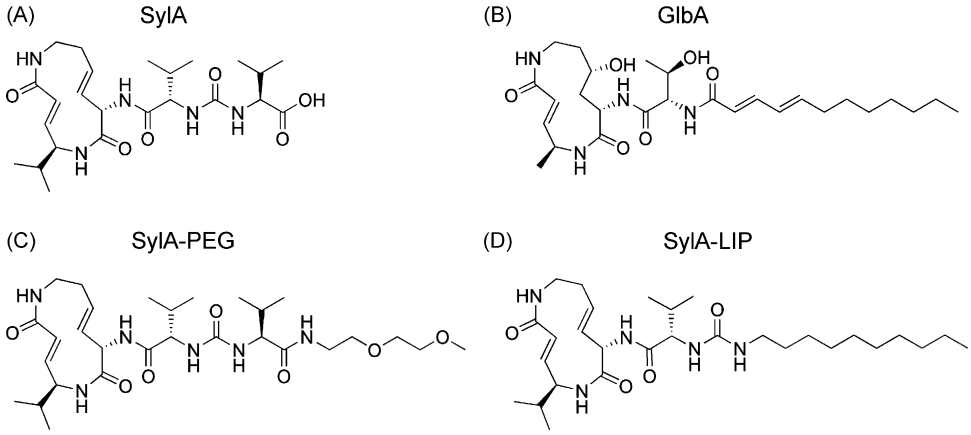

Fig. 1. Chemical structures of syrbactins, a new class of proteasome inhibitors. (A) Syringolin A (SylA) is produced by the plant pathogen *Pseudomonas syringae* pv. *syringae* (*Pss*) (MW 493.5964). (B) Glidobactin A (GlbA) is produced by an unknown species of the order *Burkholderiales* which is referred to as strain K481-B101 (ATCC 53080) (MW 520.66). (C) Pegylated SylA (SylA-PEG) is a synthetic analog of SylA which contains a pegylated moiety (MW 594.7433). (D) Lipidated SylA (SylA-LIP) is a synthetic analog of SylA which contains a lipophilic moiety (MW 533.7463).

natural products which are structurally distinct from known proteasome inhibitors [4,11]. While SylA is produced by the plant pathogen *Pseudomonas syringae* pv. *syringae* (*Pss*), GlbA is produced by an unknown species of the order *Burkholderiales* [12,13]. Remarkably, despite their difference in origin, the structural cores of SylA and GlbA are nearly identical and consist of a 12-membered ring system; however, GlbA contains a lipophilic tail which is missing in SylA (Fig. 1). The crystal structures of both SylA and GlbA in complex with the yeast proteasome revealed a novel mechanism of covalent, irreversible binding to the catalytic subunits of the proteasome with strongest affinity for the β5 subunit conferring chymotrypsin-like proteolytic activity [10,14]. Prior to this discovery, we found that SylA inhibits cell proliferation and induces apoptosis in human neuroblastoma and ovarian cancer cells [15], thus suggesting that the observed apoptosis was linked to SylA-mediated proteasome inhibition.

To further explore the biological function of syrbactins and their potential as novel drug therapeutics, this study examined the effects of four syrbactins (SylA, GlbA, and two synthetic SylA-analogs; SylA-PEG and SylA-LIP) on cellular proliferation and proteasome activity of cancer cells, including human neuroblastoma (NB), drug-sensitive/resistant multiple myeloma cells, and ovarian cancer cells. For direct comparison, the proteasome inhibitor bortezomib was included. We further examined the role of GlbA in the induction and regulation of apoptosis and autophagy. The results provide a strong rationale for the further exploration of this new proteasome inhibitor class and suggest that syrbactins are potential drug candidates for cancer therapy.

2. Materials and methods

2.1. Purification and synthesis of syrbactins

Syringolin A (SylA) and glidobactin A (GlbA) were isolated from their biological sources as described [12,16,17]. Lyophilized SylA was dissolved in sterile water and lyophilized GlbA was dissolved in sterile DMSO. Synthetic SylA (used in Fig. 2) and SylA-LIP were synthesized as previously described [18] and dissolved in DMSO. SylA-PEG was synthesized from synthetic SylA by coupling of the corresponding amino PEG residue to its C-terminal carboxylic moiety.

2.2. Mammalian cell cultures and reagents

The following panel of chemosensitive and chemoresistant cancer cell lines was used in this study. The human NB cell line SK-N-SH (N/S-type, *MYCN*-non-amplified, p53 wild type) was established from the bone marrow of a 4-year-old female patient and obtained from the American Type Culture Collection (ATCC) [19]. NB cell line SK-N-BE(2c) (I-type, *MYCN*-amplified, p53 mutant) was derived from the bone marrow of a 2-year-old male patient with progressive NB following treatment with radiotherapy and chemotherapy and was provided by B. Spengler (Fordham University) [20]. Cell lines MM1.S and MM1.RL derived from the parent cell line MM.1, which was established from peripheral blood of a multiple myeloma patient who had become resistant to steroid-based therapy. MM1.S and MM.1RL are sensitive and resistant to dexamethasone, respectively. Together, they provide critical information about disease progression, development of drug resistance, and are useful in the discovery of new therapeutics. U266 is an IL-6 producing cell line isolated from the peripheral blood of a male myeloma patient. All myeloma cells were provided by N. Krett (Northwestern University) [21]. The human ovarian cancer cell line SKOV-3 (p53 deficient, constitutively activated PI3-K and Akt/PKB), which is resistant to several cytotoxic drugs, was provided by B. Warn-Cramer (Cancer Research Center of Hawaii) [22,23]. Cells were seeded 18–24 h before syrbactin or bortezomib treatments and analyzed after 24–72 h. Bortezomib was purchased from LC Laboratories (Woburn, MA, USA). The PI3 kinase inhibitor 3-methyladenine (3-MA) also inhibits autophagic sequestration [24–26] and was from Sigma-Aldrich (St. Louis, MO, USA). Lipofectamine 2000 was used for cell transfections according to the manufacturer's protocol (Invitrogen).

2.3. Cell proliferation assay

The CellTiter 96 Aqueous One solution Cell Proliferation Assay (2-(4,5-dimethylthiazol-2-yl)-5-(3-carboxymethoxyphenyl)-2-(4-sulfophenyl)-2H-tetrazolium, inner salt; MTS) (Promega, San Luis Obispo, CA, USA) measures metabolic cell activity and was used to indirectly determine the viability of cells after 48 h treatment with SylA, GlbA, SylA-PEG, SylA-LIP or bortezomib at indicated concentrations by measuring the absorbance at 450 nm using a PerkinElmer HTS7000 Plus bioassay reader. In addition, the viability of cells was determined by counting cells using a light microscope and hemacytometer in the presence of trypan blue for exclusion of dead cells. Cytotoxicity was measured by detecting specific proteases released from damaged membranes using the Cytotox-Glo kit (Promega).

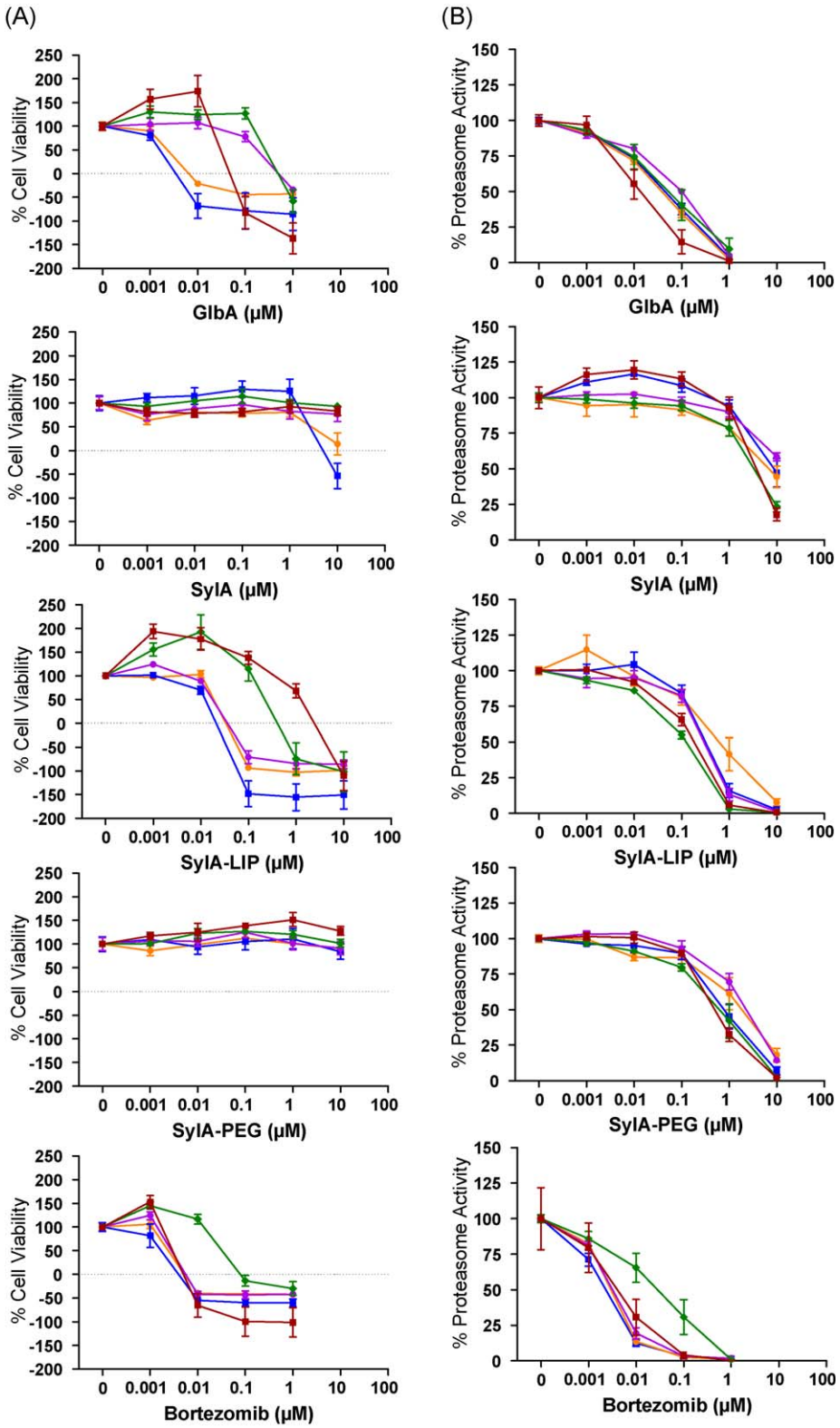

Fig. 2. Syrbactins inhibit proliferation and proteasomal activity of cancer cells. (A) A panel of human cancer cell lines including human neuroblastoma cell line SK-N-SH (red squares), human multiple myeloma cell lines MM1.S (blue squares), MM1.RL (orange circles) and U266 (purple circles), and human ovarian cancer cell line SKOV-3 (green diamonds) were treated individually over a period of 48 h with one of four syrbactins (GlbA, SylA, SylA-PEG, and SylA-LIP) at various concentrations (0–100 μM). The proteasome inhibitor bortezomib was included as a control. The viability of cells was determined by MTS assay. (B) The same cell line panel was treated individually over a period of 2 h with one of four syrbactins (GlbA, SylA, SylA-PEG, and SylA-LIP) at various concentrations (0–100 μM). The proteasome inhibitor bortezomib was included as a control. The inhibition of the chymotrypsin-like proteasome activity was determined by incubating treated cells with the luminogenic proteasome substrate, Suc-LLVY-aminoluciferin. Data normalized to controls represent the mean of three independent experiments, and each experiment was performed in duplicate ($n = 6$); bars, ±s.d. (For interpretation of the references to color in this figure legend, the reader is referred to the web version of the article.)

2.4. In vivo proteasome inhibition assay

The cell culture-based proteasome Glo™ inhibition assay was performed as previously described [10]. Solid white 96-well microtiter cell culture plates were seeded with cells as indicated and treated with syrbactin or bortezomib. Proteasome inhibition was measured using the proteasome Glo™ reagent according to the manufacturer's instructions (Promega). In brief, cancer cells were treated with SylA, GlbA, SylA-PEG, SylA-LIP or bortezomib at different concentrations as indicated and incubated for 2 h, followed by incubation for 15 min with 100 μl of proteasome Glo™ reagent, containing the bioluminescent substrate Suc-LLVY-aminoluciferin. Luminescence was then measured with a Dynex MLX luminometer.

2.5. Western blot analysis

For Western blot analysis, NB cells were seeded in 6-well cell culture plates. After 24 h, cells were incubated for 3 h with 3-MA (7.44 mM) when indicated, followed by GlbA (0.25 μM) treatment for 24 h or 0, 6, 12, 18, and 24 h for time-course experiments. Cell lysates were analyzed by sodium dodecyl sulfate-polyacrylamide gel electrophoresis (SDS-PAGE) and electro transfer to PVDF Immobilon-P membranes (Millipore, Billerica, MA, USA) as previously reported [10]. The primary antibodies were microtubule-associated protein 1 light chain 3 (LC3) and ubiquitin rabbit whole serum (Sigma, St. Louis, MO, USA), tumor suppressor protein p53 (Santa Cruz Biotechnology, Santa Cruz, CA, USA), and PARP, total Akt/PKB, phospho-Akt/PKB (Ser^{473}), and α-tubulin (Cell Signaling Technology, Danvers, MA, USA). Secondary HRP-antibodies were from GE Healthcare (Piscataway, NJ, USA). After washing the blot with deionized water, proteins were detected using the ECL Plus reagents (Amersham Biosciences, Piscataway, NJ, USA) and Kodak BioMax XAR film (Fisher Scientific, Pittsburgh, PA, USA). Membranes were stripped at 50 °C for 30 min with ECL stripping buffer (62.5 mM Tris–HCl, pH 6.7, 2% SDS, 100 mM 2-mercaptoethanol) and sequentially probed. Bands were quantified using a Bio-Rad Multi Imager and Quantity One Quantitation Software (Bio-Rad).

2.6. Microscopy

Light micrographs were taken after 24 and 48 h treatment at 10× magnification using an inverted Leica DM IL digital microscope. For visualization of endogenous LC3-II accumulation, SK-N-SH cells were treated with GlbA (0.1 μM) or vehicle (DMSO) for 24 h, followed by fixation and permeabilization in ice-cold methanol. Fixed cells were washed and incubated with LC3B antibody (Cell Signaling Technology) followed by incubation with Alexa-Fluor 488 secondary antibody (Molecular Probes, Invitrogen, Carlsbad, CA, USA). ToPro-3 was included to visualize nuclei and slides were mounted using Prolong Gold® mounting medium (Molecular Probes). For GFP-LC3 overexpression studies, SK-N-SH cells were transfected with 0.8 μg pEGFP-LC3 plasmid and prepared as described above. For co-localization studies, transfected cells were incubated with anti-ubiquitin (Cell Signaling Technology) and Alexa-Fluor 594 secondary antibody (Molecular Probes). Samples were analyzed by confocal laser scanning microscope (Leica TCS SP-5 AOBS) at 63× magnification.

3. Results

3.1. Syrbactins inhibit the proliferation of cancer cells

To examine whether the syrbactins inhibit cell proliferation, GlbA, SylA, and two synthetic SylA-analogs (SylA-PEG and SylA-LIP) were analyzed in parallel (Fig. 1). Bortezomib was included as a control for comparison as this drug represents an established proteasome inhibitor that has proven effective in the clinical setting in the treatment of patients with relapsed and/or refractory MM. Human neuroblastoma cells SK-N-SH, human multiple myeloma cells MM1.S, MM1.RL and U266 as well as human ovarian cancer cells SKOV-3 were treated with syrbactins at different concentrations, and the cell viability was determined using the MTS assay as described in Material and Methods. As shown in Fig. 2A, GlbA most effectively reduced the viability of all tested cell lines in a dose-dependent manner. GlbA was most effective in cell lines MM1.S and MM1.RL with IC_{50} values of 0.004 μM and 0.005 μM, respectively, and the least effective in SKOV-3 cells with an IC_{50} of 0.852 μM (Supplement Table 1). SylA also inhibited the cell proliferation but at significantly higher, mid micromolar concentrations as previously shown [10,15].

To determine whether the differences in activity might be due to the lipophilic moiety of GlbA which is absent in the natural form of SylA, we also tested two synthetic SylA-analogs, SylA-PEG and SylA-LIP, bearing pegylated and lipidated tails, respectively (Fig. 1C and D). Remarkably, SylA-LIP, but not SylA-PEG, was effective in all tested cell lines and most pronounced in MM cell lines (MM1.S, MM1.RL, and U266) with IC_{50} values of 0.026 μM, 0.033 μM, and 0.076 μM, respectively. In comparison, bortezomib was most effective in MM1.S and MM1.RL cells (IC_{50} values: 0.0024 μM and 0.003 μM, respectively) and the least effective in SKOV-3 cells (IC_{50}: 0.0399 μM). Collectively, the results presented in Fig. 2A (summarized in Supplement Table 1) suggest that syrbactins exhibit anti-proliferative activity but at varying concentrations. At higher concentrations, GlbA, SylA-LIP, and bortezomib also induced cytotoxicity in all cell lines as the number of viable cells was lower than at the beginning of the experiments ($T = 0$). Overall, GlbA was the most effective syrbactin and killed MM cells in a fashion comparable to bortezomib. A significant difference between SylA and SylA-LIP was observed, suggesting that the lipophilic moiety of SylA-LIP improves its anti-proliferative activity by over a 1000-fold (for example, in MM1.RL cells).

3.2. Syrbactins inhibit the proteasomal activity of cancer cells

We next tested if the four syrbactins GlbA, SylA, SylA-PEG, and SylA-LIP inhibit the proteasomal activity in metabolically active cancer cells (SK-N-SH, MM1.S, MM1.RL, U266, and SKOV-3) using a cell culture-based proteasome inhibition assay that measures the degradation of a luminogenic substrate (Suc-LLVY-aminoluciferin) specific for the chymotryptic-like proteolytic activity of the proteasome.

As shown in Fig. 2B, GlbA inhibited the proteasomal activity of all cell lines in a dose-dependent manner. SK-N-SH cells were most sensitive to GlbA treatment with an IC_{50} of 0.015 μM (Supplement Table 2). SylA also inhibited the proteasome activity of all tested cell lines in a dose-dependent manner, but at significantly higher (~45–300-fold) concentrations than GlbA. While SylA-LIP, and less so SylA-PEG, improved their respective activities compared to SylA, they exhibited lower activities compared to GlbA. Bortezomib inhibited all cell lines in a dose-dependent manner with IC_{50} values in the low nanomolar range, except for SKOV-3 cells where the IC_{50} was about 10-fold higher and thus comparable to GlbA. Together, the data suggest that GlbA is the most potent syrbactin with highest anti-proteasomal activity in SK-N-SH cells.

3.3. Syrbactin treatment leads to accumulation of ubiquitinated proteins in neuroblastoma cells

Ubiquitin is a highly conserved 76-amino acid protein, and proteins that are recognized by the 26S proteasome are typically

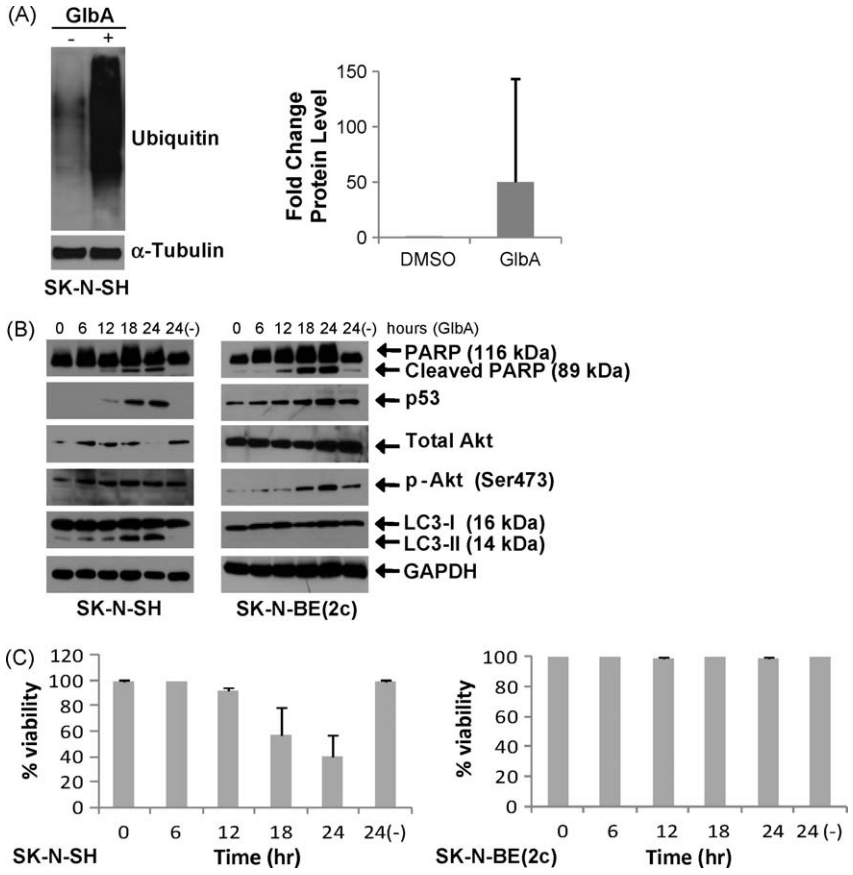

Fig. 3. Syrbactin treatment leads to accumulation of ubiquitinated proteins. Proteasome inhibition resulted in the accumulation of ubiquitinated proteins in lysates of human neuroblastoma SK-N-SH cells as shown by Western blot analysis using a rabbit serum that recognizes endogenous ubiquitin. (A) Cells were treated with 0.25 μM GlbA, and control samples were treated with vehicle DMSO for 24 h. Ubiquitinated proteins were quantified using the BioRad Quantity One software, shown by graphical representation. Data represent the mean of three independent experiments ($n = 3$); bars, ±s.d. (B) SK-N-SH and SK-N-BE(2c) cells were treated with 0.25 μM GlbA for 0, 6, 12, 18, and 24 h and control samples were treated with vehicle DMSO. Western blot analyses of cell lysates revealed the induction of apoptosis as judged by PARP cleavage and p53 accumulation. The phosphorylation of Akt/PKB at Ser^{473} was observed. In addition, the lipidated form of LC3, LC3-II, was observed in GlbA-treated cells. Data represent three independent experiments ($n = 3$). (C) The membrane integrity and viability of these cells was also determined by trypan blue exclusion. GlbA induced a loss of membrane integrity and viability in SK-N-SH cells but not SK-N-BE(2c) cells. Data represent the mean of three independent experiments ($n = 3$); bars, ±s.d.

conjugated to a poly-ubiquitin chain before degradation. We therefore hypothesized that proteasome inhibition should lead to the accumulation of cellular proteins that are ubiquitinated. Since the GlbA-mediated proteasome inhibition was most potent in NB cells, we next analyzed cell lysates of GlbA-treated or vehicle-treated control SK-N-SH cells by Western blot using a rabbit serum which recognizes ubiquitinated proteins. GlbA-treated cells showed a marked increase in ubiquitinated cellular proteins compared to untreated control cells (Fig. 3A). We previously observed that SylA treatment also leads to the accumulation of ubiquitinated proteins [10]; however, GlbA induced comparable effects at a 100-fold lower concentration (Fig. 3A). These results are in support of our observation that syrbactins inhibit the proteasome in metabolically active cells, and that GlbA is a more potent inhibitor than SylA.

3.4. Syrbactins induce apoptosis in neuroblastoma cells

Previous studies have shown that inhibition of ubiquitin-mediated degradation of proteins through the ubiquitin-proteasome pathway leads to the onset of apoptosis. Therefore, we determined whether syrbactin-promoted cell death involved the induction of apoptosis. SK-N-SH and SK-N-BE(2c) cells were treated with GlbA for various times over a 24-h period. First, we probed cell lysates for the presence of PARP cleavage, which is indicative of apoptosis [27]. As shown in Fig. 3B, GlbA-treated cells contained cleaved PARP (89 kDa) within 12 h of drug treatment, while only non-cleaved PARP (116 kDa) was detected at earlier time points and in control cells.

The tumor suppressor protein p53 is regulated by proteasome degradation and plays a key role during apoptosis. Therefore, we next focused our attention at total levels of p53 in cell lysates. The accumulation of p53 was detected in GlbA-treated cell lysates within 12 h of treatment (Fig. 3B). In addition to p53, we also examined the presence and activation of Akt/PKB, a well-characterized anti-apoptotic protein kinase. GlbA induced Ser^{473} phosphorylation of Akt/PKB within 18 h of treatment (Fig. 3B), suggesting that GlbA activates Akt/PKB and thus exhibits an opposing effect which may counteract apoptosis.

The trypan blue exclusion assay confirmed that within 18 h of GlbA treatment there was a loss of membrane integrity and viability in SK-N-SH cells (Fig. 3C). Interestingly, GlbA did not affect the viability of SK-N-BE (2c) cells within the 24-h period (Fig. 3C), despite the presence of PARP cleavage.

Treatment with GlbA also induced morphological changes in NB cells (Fig. 4A). While untreated SK-N-SH control cells were triangular-shaped, GlbA-treated cells appeared rounded and partially detached from the culture plates at 24 h, with more extensive morphological changes at 48 h. These morphological changes are characteristic for cells that undergo apoptosis.

To further explore our observations, we analyzed GlbA-treated SK-N-SH cells with or without 3-methyladenine (3-MA), an

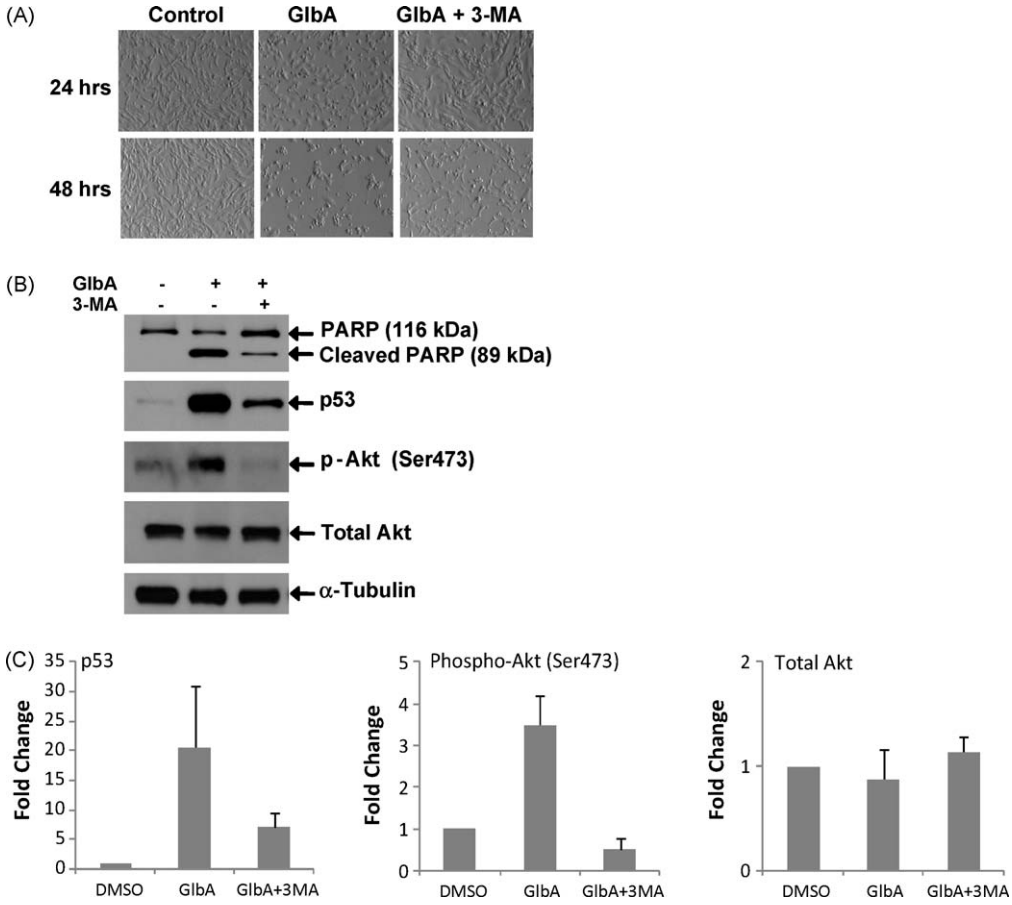

Fig. 4. Treatment of neuroblastoma cells with GlbA induces apoptosis. (A) SK-N-SH cells at 10× magnification after treating with DMSO (control, left), GlbA (0.25 μM, middle) or GlbA + 3-MA (7.44 mM, right) for 24 and 48 h. GlbA treatment produced rounded cells that partially detached from the cell culture dish, while control cells remained triangle-shaped and adherent to the surface. (B) Analysis of GlbA-treated cells after 24 h of treatment revealed the induction of apoptosis as judged by PARP cleavage and p53 accumulation using Western blot analysis. In addition, phosphorylation of Akt/PKB at Ser^{473} was observed, while total Akt/PKB protein levels remained unchanged. Treatment of cells with class III PI3K inhibitor 3-methyladenine (3-MA) partially reverted PARP cleavage and p53 accumulation, and fully prevented Akt/PKB phosphorylation. (C) Protein p53, phospho-Akt/PKB (Ser^{473}), and total Akt/PKB were quantified using the BioRad Quantity One software, shown by graphical representation. Data represent the mean of three independent experiments ($n = 3$); bars, ±s.d.

inhibitor of PI3-kinase [24–26], and probed cell lysates after 24 h for the presence of PARP cleavage. As shown in Fig. 4B, GlbA-treated cells contained large quantities of cleaved PARP (89 kDa), while only non-cleaved PARP (116 kDa) was detected in control cells. Interestingly, the presence of 3-MA partially prevented the cleavage of PARP.

GlbA treatment led to a strong accumulation of p53 in cellular lysates compared to control cells and 3-MA partially reduced this accumulation (Fig. 4B). While the total Akt/PKB protein levels did not significantly change, we noted an increase of Ser^{473}-phosphorylated Akt/PKB in response to GlbA treatment. This phosphorylation of Ser^{473} was prevented by co-treatment with 3-MA (Fig. 4B). Together, the results support the time-course experiments of Fig. 3B and suggest that GlbA induces p53 accumulation and promotes apoptosis in SK-N-SH cells, but also activates Akt/PKB, and this activation can be prevented by treatment with 3-MA.

3.5. Syrbactins-induced proteasome inhibition promotes autophagy in neuroblastoma cells

Proteasome degradation and autophagy are the two main proteolytic pathways used by cells to degrade cellular proteins. Since the treatment of cells with 3-MA results in the inhibition of autophagy [28] and 3-MA reduces the effects of GlbA treatment (Fig. 4), we were curious to determine whether syrbactins induce autophagy. To test this hypothesis, we probed GlbA-treated SK-N-SH cells for the presence of native microtubule-associated protein 1 light chain 3 (LC3) protein. Untreated control cells primarily contain non-lipidated form of LC3 (LC3-I; 18 kDa), while autophagic cells accumulate a lipidated form of LC3 (LC3-II; 16 kDa), which associates with autophagic vacuoles (autophagosomes) and thus presents a reliable marker of autophagy [29]. As illustrated in Fig. 5A, we found that GlbA-treated cells accumulated native LC3-II when compared to untreated control cells and the co-treatment of cells with 3-MA reverted the GlbA-induced formation of LC3-II. The lipidation of LC3-I into LC3-II occurred within 12–18 h of GlbA treatment in SK-N-SH cells, but not SK-N-BE(2c) cells (Fig. 3B). The formation of distinct autophagosomes was also detected by immunofluorescence in GlbA-treated SK-N-SH cells as represented by green puncta which were absent from untreated control cells (Fig. 5B).

Consistent with these findings, cells transfected with a GFP-LC3 construct exhibited a transition of the GFP-LC3 signals from a diffuse cytoplasmic pattern to a punctated membrane pattern following the treatment with GlbA (Fig. 6A), suggesting the localization of LC3 to autophagosomes. Similar GFP-LC3 puncta were observed in the presence of rapamycin, an mTOR inhibitor that has been shown to induce autophagy. We also found by confocal microscopic analysis that these autophagosome representing GFP-LC3 puncta co-localize with ubiquitinated aggregates (Fig. 6B) and similar observations were made by others in

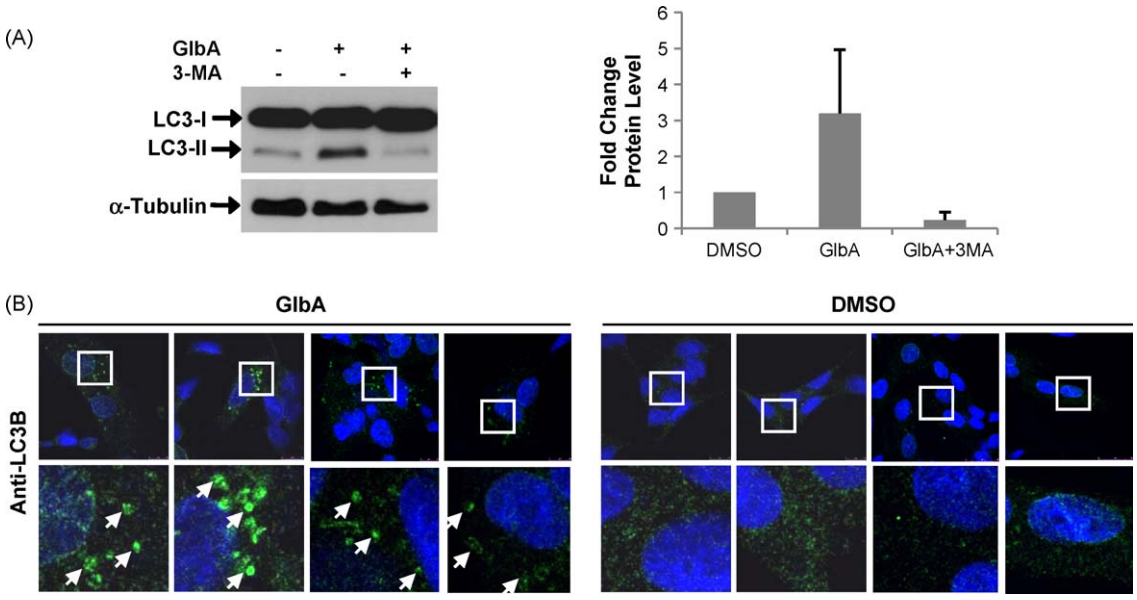

Fig. 5. Treatment of human neuroblastoma cells with GlbA promotes autophagy. (A) SK-N-SH cells were treated with GlbA (0.25 μM) for 24 h in the absence or presence of PI3K inhibitor 3-methyladenine (3-MA), a known inhibitor of autophagy, and probed for the presence of native microtubule-associated protein 1 light chain 3 (LC3) protein using LC3 antibody (Sigma) and Western blot analysis. LC3-II, a 16 kDa (lipidated) form associated with autophagosomes, was present only in lysates of GlbA-treated cells, but not in DMSO or 3-MA-treated control cells. Alpha-tubulin was used as loading control. LC3-II was quantified using the BioRad Quantity One software, shown by graphical representation. Data represent the mean of three independent experiments ($n = 3$); bars, ±s.d. (B) The LC3B antibody (Cell Signaling Technology) was used to detect autophagosomes by immunofluorescence microscopy in SK-N-SH cells. Autophagosomes were present in GlbA (0.1 μM)-treated cells and absent in vehicle (DMSO)-treated cells. The white squares in the low power images (upper panels) are magnified (lower panels) and selected autophagosomes are highlighted by white arrows. Four images per treatment are shown. Data are representative of three independent experiments ($n = 3$).

GFP-LC3-expressing prostate cancer cells in response to bortezomib [30].

Together, these experiments suggest that GlbA, in addition to inducing apoptosis, also promotes autophagy. Moreover, autophagy could participate in the clearance of ubiquitinated protein aggregates which have accumulated in response to proteasome inhibition.

4. Discussion

The proteasome has recently been recognized as a target for anticancer therapy. Numerous studies successfully showed that proteasome inhibitors preferentially kill cancer cells and induce apoptosis without affecting non-transformed cells [31]. The most prominent inhibitor, bortezomib, has been approved by the FDA for the treatment of relapsed/refractory multiple myeloma and mantle cell lymphoma, and three second generation proteasome inhibitors, carfilzomib (PR-171), salinosporamide A (NPI-0052), and CEP-18770 are in phase I and phase II clinical trials [9,32,33].

Remarkably, a number of proteasome inhibitors are natural products including lactacystin, epoxomicin, salinosporamide A, eponemycin, tyropeptin A, and TMC-95, and six major families based on the chemical mechanism have been identified [4]. We have recently made the discovery of a seventh class of proteasome inhibitors, the syrbactins, which are structurally distinct natural products that bind the proteasome by a unique mechanism [4,10,11].

Syrbactins so far include the syringolins and glidobactins. Although they share similar structural features, they differ in their macrocyclic lactam core structure and exocyclic side chain. We recently described the total synthesis of SylA and also of SylB, one of several minor metabolites produced by the plant pathogen *Pss* [18]. SylB has strong structural similarity to SylA and differs from SylA only by the substitution of the SylA 3,4-dehydrolysine residue with a lysine moiety, which results in an alternative scaffold structure with less ring strain [18]. While more distinct, glidobactins are structurally related to syringolins (Fig. 1) and have been discovered in the late 1980s [34–36], however, the mode of action was not recognized until recently [10]. In our previous work, we showed that *in vitro*, GlbA is the most potent syrbactin proteasome inhibitor identified so far and is 15-fold more active than SylA for the chymotryptic and the tryptic proteasome activity. In contrast, GlbA did not inhibit the caspase-like activity while SylA and SylB moderately affected this activity and this observation was confirmed by co-crystallization [10,18]. As anticipated, the rationally designed syringolin A-based lipophilic derivative (SylA-LIP; Fig. 1D) proved to be about 100-fold more potent than SylA in its ability to inhibit the chymotryptic activity of the proteasome *in vitro* [18].

In this report, we confirmed our previous *in vitro* findings with SylA and provide strong evidence that GlbA, and also SylA-LIP inhibit cell proliferation and proteasomal activity at significantly lower concentrations than SylA when applied to intact, metabolically active cancer cells. Using a cell-based proteasome activity assay, we observed that GlbA was up to 300-fold more active than SylA depending on the cell type with highest/lowest activities in SK-N-SH cells and U266 cells, respectively. SylA-LIP was up to 48-fold more active than SylA with highest/lowest activities in SKOV-3 and MM1.RL, respectively (Supplement Table 2). Interestingly, SylA and SylA-PEG had little effect on cell viability but inhibited the proteasomal activity. This observation suggests that SylA and SylA-PEG do not easily pass the cell membrane which remains intact when exposed to the MTS assay reagents. In contrast, cells exposed to the proteasome assay reagents are permeablized at the end of the 2-h incubation period. Therefore, it is possible that in the proteasome assay, SylA and SylA-PEG do not enter the cell during the 2-h incubation period but after cell permeabilization. Indeed, proteasome activity experiments in which GlbA- and SylA-treated cells were washed (in order to remove the inhibitor) after a 2, 12 or 24-h incubation period (before permeabilization) confirmed that lipophilic GlbA enters cells more readily during the incubation period than hydrophilic SylA (Supplement Fig. 1). Similarly, this

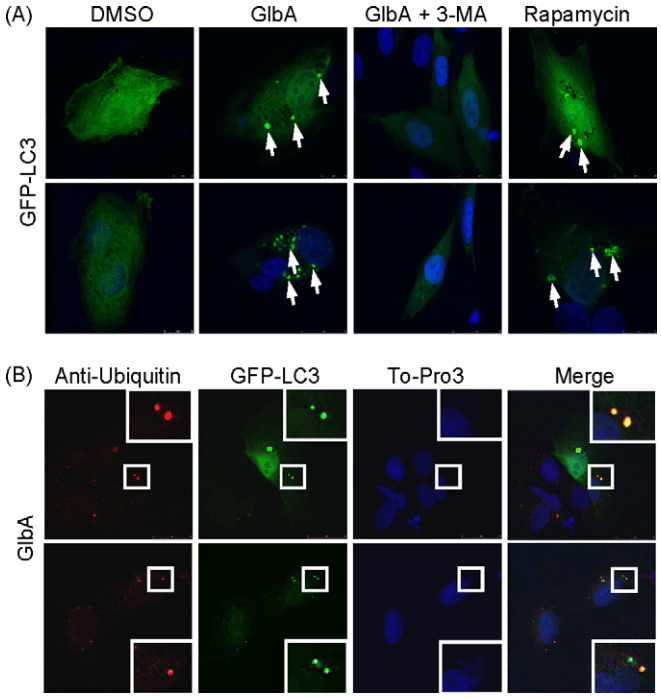

Fig. 6. GlbA induces the formation of autophagosomes. (A) Human neuroblastoma cells SK-N-SH expressing GFP-LC3 were treated with GlbA (0.1 μM) for 24 h in the absence or presence of PI3K inhibitor 3-methyladenine (3-MA), a known inhibitor of autophagy. Rapamcyin (0.25 μM) was used as a positive control. Distinct autophagosomes (green puncta, indicated by white arrows) were present in GlbA-treated cells as well as rapamycin-treated (positive control) cells but were absent in vehicle (DMSO)-treated (negative control) cells. (B) SK-N-SH cells expressing GFP-LC3 were treated with GlbA (0.1 μM) for 24 h and cells immunostained with an anti-ubiquitin rabbit serum. Cells were then subjected to confocal microscopy. Red puncta show ubiquitin-positive autophagosomes, green puncta represent GFP-LC3 autophagosomes, and merged images indicate distinct sites of co-localization (yellow). To-Pro3 was used to visualize nuclei (blue). Cells in the white squares of the low power images are magnified (inlets). Two images per treatment are shown. Data are representative of three independent experiments ($n = 3$). (For interpretation of the references to color in this figure legend, the reader is referred to the web version of the article.)

may explain why SylA-PEG was effective in the proteasome assay but not in the cell viability assay.

We further examined these effects by analyzing whole cell lysates from GlbA-treated and untreated cells by Western blot analysis. To study signaling proteins that are regulated towards the beginning of apoptosis, we treated SK-N-SH cells for designated times up to 24 h, since longer treatment at 48 h typically resulted in a non-specific, total degradation of cellular proteins. Western blot analyses revealed that GlbA induced PARP cleavage, a typical marker for apoptosis, and led to p53 accumulation, a protein known to be involved in the induction of apoptosis. These findings were consistent with our previous study on SylA treatment of cancer cells [10,15]. While GlbA treatment had little effect on total Akt/PKB protein levels, the phosphorylation of Akt/PKB at residue Ser^{473} increased significantly, thus suggesting the activation of Akt/PKB.

Interestingly, co-treatment with 3-MA reduced or prevented the GlbA-induced cellular effects (Fig. 4). In addition, co-treatment with 3-MA attenuated the cytotoxic effects of GlbA (Supplement Fig. 2). GlbA also increased the lipidated form of LC3 (LC3-II) as well as the number of autophagosomes in GlbA-treated cells, indicating the onset of autophagy. Together, these findings suggest that GlbA-mediated inhibition of proteasomal degradation activates both apoptosis and autophagy. Inhibition of autophagy decreased the cytotoxic effects of GlbA and decreased PARP cleavage after 24 h, supporting a pro-apoptotic role of autophagy during GlbA induced proteasome inhibition. Conversely, the onset of autophagy may be a compensatory mechanism in response to GlbA-induced proteasome inhibition, as observed by the co-localization of ubiquitin with LC3-containing autophagosomes. Indeed, Ding et al. suggested that autophagy is likely activated in response to endoplasmic reticulum stress caused by misfolded proteins during proteasome inhibition [30]. The PI3K/Akt signaling has been associated with both anti-apoptotic and pro-apoptotic responses [37–39] and, similar to our observation, bortezomib was found to activate Akt/PKB *in vitro* and in treated prostate cancer tissues [40]. In our study, the 3-MA effect on Akt/PKB activation during GlbA treatment supports a pro-apoptotic role for Akt/PKB, however, Akt/PKB activation may also occur as a compensatory response to the induction of apoptosis. The results clearly show that GlbA is able to induce both apoptosis and autophagy in neuroblastoma cells. However, it is not clear whether the induction of autophagy is a pro-survival or pro-cell death response.

In summary, our study introduces a new class of proteasome inhibitors, the syrbactins, and provides evidence for their use as anti-proliferative agents that exhibit apoptotic properties. Although bortezomib is a successful drug that is used in the treatment of MM and currently evaluated in clinical trials for effectiveness in other types of cancer, novel proteasome inhibitors are needed due to the occurrence of toxicities and the development of potential drug resistance associated with prolonged treatments. Proteasome inhibitors are also known to sensitize chemoresistant cells, further underlining their importance of this new class of therapeutics. Therefore, the newly discovered syrbactin class of proteasome inhibitors should be further studied and developed into a therapeutic agent that may be used for combination treatments or as second-line therapy in bortezomib-resistant tumors.

Acknowledgments

This work was supported by a career development grant and institutional funds from the Cancer Research Center of Hawaii (A.S.B.) and by the Swiss National Science Foundation grant 3100A0-100046 (R.D.). C.R.A. was in part supported by the Cell and Molecular Biology Graduate Program of the University of Hawaii. We thank Dr. David J. Feith (Pennsylvania State University, Hershey, PA) and Dr. Dirk Geerts (University of Amsterdam, The Netherlands) for critical review of the manuscript. We are also grateful to Nancy L. Krett (Northwestern University, Chicago, IL) for providing multiple myeloma cells, Dr. Bonnie Warn-Cramer (Cancer Research Center of Hawaii, Honolulu, HI) for SKOV-3 cells, Dr. Barbara Spengler (Fordham University, Bronx, NY, USA) for SK-N-BE(2c) cells, and Dr. Tamotsu Yoshimori (Research Institute for Microbial Diseases, Osaka University, Osaka, Japan) for plasmid pEGFP-LC3. Dr. Tamas Borsics, Dr. Vivian Su, and Lisette P. Yco are thanked for excellent technical assistance.

Appendix A. Supplementary data

Supplementary data associated with this article can be found, in the online version, at doi:10.1016/j.bcp.2010.03.031.

References

[1] Adams J. The proteasome: structure, function, and role in the cell. Cancer Treat Rev 2003;29(Suppl. 1):3–9.
[2] Kisselev AF, Goldberg AL. Proteasome inhibitors: from research tools to drug candidates. Chem Biol 2001;8:739–58.
[3] Adams J. The proteasome: a suitable antineoplastic target. Nat Rev Cancer 2004;4:349–60.
[4] Kisselev AF. Joining the army of proteasome inhibitors. Chem Biol 2008;15:419–21.

[5] Rajkumar SV, Richardson PG, Hideshima T, Anderson KC. Proteasome inhibition as a novel therapeutic target in human cancer. J Clin Oncol 2005;23:630–9.
[6] Voorhees PM, Dees EC, O'Neil B, Orlowski RZ. The proteasome as a target for cancer therapy. Clin Cancer Res 2003;9:6316–25.
[7] Bachmann AS. Proteasome inhibitors in pediatric cancer treatment. Hawaii Med J 2008;67:247–9.
[8] Mikhael JR, Belch AR, Prince HM, Lucio MN, Maiolino A, Corso A, et al. High response rate to bortezomib with or without dexamethasone in patients with relapsed or refractory multiple myeloma: results of a global phase 3b expanded access program. Br J Haematol 2009;144:169–75.
[9] Chauhan D, Catley L, Li G, Podar K, Hideshima T, Velankar M, et al. A novel orally active proteasome inhibitor induces apoptosis in multiple myeloma cells with mechanisms distinct from Bortezomib. Cancer Cell 2005;8:407–19.
[10] Groll M, Schellenberg B, Bachmann AS, Archer CR, Huber R, Powell TK, et al. A plant pathogen virulence factor inhibits the eukaryotic proteasome by a novel mechanism. Nature 2008;452:755–8.
[11] Moore BS, Eustaquio AS, McGlinchey RP. Advances in and applications of proteasome inhibitors. Curr Opin Chem Biol 2008;12:434–40.
[12] Schellenberg B, Bigler L, Dudler R. Identification of genes involved in the biosynthesis of the cytotoxic compound glidobactin from a soil bacterium. Environ Microbiol 2007;9:1640–50.
[13] Wäspi U, Blanc C, Winkler C, Ruedi P, Dudler R. Syringolin, a novel peptide elicitor from *Pseudomonas syringae* pv. syringae that induces resistance to Pyricularia oryzae in rice. Mol Plant Microbe Interact 1998;11:727–33.
[14] Clerc J, Florea BI, Kraus M, Groll M, Huber R, Bachmann AS, et al. Syringolin A selectively labels the 20 S proteasome in murine EL4 and wild-type and bortezomib-adapted leukaemic cell lines. Chembiochem 2009;10:2638–43.
[15] Coleman CS, Rocetes JP, Park DJ, Wallick CJ, Warn-Cramer BJ, Michel K, et al. Syringolin A, a new plant elicitor from the phytopathogenic bacterium *Pseudomonas syringae* pv. syringae, inhibits the proliferation of neuroblastoma and ovarian cancer cells and induces apoptosis. Cell Prolif 2006;39:599–609.
[16] Amrein H, Makart S, Granado J, Shakya R, Schneider-Pokorny J, Dudler R. Functional analysis of genes involved in the synthesis of syringolin A by *Pseudomonas syringae* pv. syringae B301 D-R. Mol Plant Microbe Interact 2004;17:90–7.
[17] Wäspi U, Schweizer P, Dudler R. Syringolin reprograms wheat to undergo hypersensitive cell death in a compatible interaction with powdery mildew. Plant Cell 2001;13:153–61.
[18] Clerc J, Groll M, Illich DJ, Bachmann AS, Huber R, Schellenberg B, et al. Synthetic and structural studies on syringolin A and B reveal critical determinants of selectivity and potency of proteasome inhibition. Proc Natl Acad Sci USA 2009;106:6507–12.
[19] Biedler JL, Helson L, Spengler BA. Morphology and growth, tumorigenicity, and cytogenetics of human neuroblastoma cells in continuous culture. Cancer Res 1973;33:2643–52.
[20] Biedler JL, Roffler-Tarlov S, Schachner M, Freedman LS. Multiple neurotransmitter synthesis by human neuroblastoma cell lines and clones. Cancer Res 1978;38:3751–7.
[21] Greenstein S, Krett NL, Kurosawa Y, Ma C, Chauhan D, Hideshima T, et al. Characterization of the MM.1 human multiple myeloma (MM) cell lines: a model system to elucidate the characteristics, behavior, and signaling of steroid-sensitive and -resistant MM cells. Exp Hematol 2003;31:271–82.
[22] Fogh J, Trempe G. New human tumor cell lines. In: Fogh J, editor. Human tumor cells in vitro. New York: Plenum Press; 1975. p. 155.
[23] Fogh J, Wright WC, Loveless JD. Absence of HeLa cell contamination in 169 cell lines derived from human tumors. J Natl Cancer Inst 1977;58:209–14.
[24] Blommaart EF, Krause U, Schellens JP, Vreeling-Sindelarova H, Meijer AJ. The phosphatidylinositol 3-kinase inhibitors wortmannin and LY294002 inhibit autophagy in isolated rat hepatocytes. Eur J Biochem 1997;243:240–6.
[25] Ito S, Koshikawa N, Mochizuki S, Takenaga K. 3-Methyladenine suppresses cell migration and invasion of HT1080 fibrosarcoma cells through inhibiting phosphoinositide 3-kinases independently of autophagy inhibition. Int J Oncol 2007;31:261–8.
[26] Wu YT, Tan HL, Shui G, Bauvy C, Huang Q, Wenk MR, et al. Dual role of 3-methyladenine in modulation of autophagy via different temporal patterns of inhibition on class I and III phosphoinositide 3-kinase. J Biol Chem 2010;285:10850–61.
[27] Duriez PJ, Shah GM. Cleavage of poly(ADP-ribose) polymerase: a sensitive parameter to study cell death. Biochem Cell Biol 1997;75:337–49.
[28] Qin ZH, Wang Y, Kegel KB, Kazantsev A, Apostol BL, Thompson LM, et al. Autophagy regulates the processing of amino terminal huntingtin fragments. Hum Mol Genet 2003;12:3231–44.
[29] Tanida I, Ueno T, Kominami E. LC3 conjugation system in mammalian autophagy. Int J Biochem Cell Biol 2004;36:2503–18.
[30] Ding WX, Ni HM, Gao W, Yoshimori T, Stolz DB, Ron D, et al. Linking of autophagy to ubiquitin-proteasome system is important for the regulation of endoplasmic reticulum stress and cell viability. Am J Pathol 2007;171:513–24.
[31] Orlowski RZ, Kuhn DJ. Proteasome inhibitors in cancer therapy: lessons from the first decade. Clin Cancer Res 2008;14:1649–57.
[32] Demo SD, Kirk CJ, Aujay MA, Buchholz TJ, Dajee M, Ho MN, et al. Antitumor activity of PR-171, a novel irreversible inhibitor of the proteasome. Cancer Res 2007;67:6383–91.
[33] Piva R, Ruggeri B, Williams M, Costa G, Tamagno I, Ferrero D, et al. CEP-18770: A novel, orally active proteasome inhibitor with a tumor-selective pharmacologic profile competitive with bortezomib. Blood 2008;111:2765–75.
[34] Oka M, Nishiyama Y, Ohta S, Kamei H, Konishi M, Miyaki T, et al. Glidobactins A, B and C, new antitumor antibiotics. I. Production, isolation, chemical properties and biological activity. J Antibiot 1988;41:1331–7.
[35] Oka M, Ohkuma H, Kamei H, Konishi M, Oki T, Kawaguchi H. Glidobactins D, E, F, G and H; minor components of the antitumor antibiotic glidobactin. J Antibiot 1988;41:1906–9.
[36] Oka M, Yaginuma K, Numata K, Konishi M, Oki T, Kawaguchi H. Glidobactins A, B and C, new antitumor antibiotics. II. Structure elucidation. J Antibiot 1988;41:1338–50.
[37] Maddika S, Ande SR, Wiechec E, Hansen LL, Wesselborg S, Los M. Akt-mediated phosphorylation of CDK2 regulates its dual role in cell cycle progression and apoptosis. J Cell Sci 2008;121:979–88.
[38] Maddika S, Bay GH, Kroczak TJ, Ande SR, Wiechec E, Gibson SB, et al. Akt is transferred to the nucleus of cells treated with apoptin, and it participates in apoptin-induced cell death. Cell Prolif 2007;40:835–48.
[39] van Gorp AG, Pomeranz KM, Birkenkamp KU, Hui RC, Lam EW, Coffer PJ. Chronic protein kinase B (PKB/c-akt) activation leads to apoptosis induced by oxidative stress-mediated Foxo3a transcriptional up-regulation. Cancer Res 2006;66:10760–9.
[40] Ayala G, Yan J, Li R, Ding Y, Thompson TC, Mims MP, et al. Bortezomib-mediated inhibition of steroid receptor coactivator-3 degradation leads to activated Akt. Clin Cancer Res 2008;14:7511–8.